MODELING MINERAL DUST EVENT FREQUENCIES FROM CHINESE DESERTS

LAURENT Benoit (1), MARTICORENA Béatrice (1), CHAZETTE Patrick (2), SCHMECHTIG Catherine (1), and MAIGNAN Fabienne (2)

(1)LISA, Universités P7-P12, UMR CNRS 7583, Créteil, France, (2) LSCE, UMR CEA-CNRS 1572, Saclay, France.

blaurent@lisa.univ-paris12.fr

1. INTRODUCTION

Mineral dust is one of the main sources of tropospheric aerosol. The amount of mineral dust, resulting from the aeolian erosion in the arid and semi-arid areas of the Earth, injected in the troposphere was estimated to ~ 2000Tg.y^{-1}, ~40% of the global annual amount of aerosol emitted each year in the atmosphere (IPCC, 2001). From the estimated deposition fluxes over the ocean (Duce, 1995), it appears that the Chinese deserts are one of the main sources of mineral dust in the world. Arid and semi arid areas in China represent 3 millions km², i.e. 1/3 of the Chinese territory (Mainguet, 1996). The desert areas are mainly composed of sandy (*shamo*) or stony surfaces (*gobi*) (Mainguet, 1996). Most of these deserts are located in closed basins, resulting in a specific air circulation. Moreover, dust emissions exhibit a clear seasonal cycle characterized by a maximum in spring (highest wind velocity and low precipitation) and a minimum in winter (lowest wind velocity) (Parungo et al., 1994).

2. MAPPING THE AERODYNAMIC ROUGHNESS LENGTH

Dust emission is a sporadic process, due to the existence of a **wind velocity threshold** for aeolian erosion. This threshold depends both on the soil size distribution and on the surface roughness. It controls the dust events frequency, i.e. the number of times the wind velocity is higher than the erosion threshold, and it influences the dust flux intensity, which depends on how much the threshold is exceeded.

Marticorena and Bergametti [1995] have developed a dust emission model including a parameterization of the threshold wind friction velocity U*t as a function of the **aerodynamic roughness length Z_0**. Based on this model, the simulation of the frequency of desert dust events requires a **map of aerodynamic roughness length.**

2.1 Surface roughness and remote sensing

Remote sensing offers the opportunity to use daily and global data sets used for the study of surface properties. The semi-empirical model of Roujean [1991] is used in the POLDER processing line to retrieve the Bidirectional Reflectance Distribution Function. The so-called **protrusion coefficient ($PC=k_1/k_0$)** derived from the POLDER BRDF is well suited to estimate the surface roughness (Roujean et al., 1992).

The characteristics of the available POLDER data set are :

- 8 months of data (Nov 96 to Jun 97)
- Global coverage
- Resolution of the POLDER pixel : *~6 km x 6 km, ~1/16°*
- Daily passage of the satellite over a pixel for 10 to 15 viewing angles → determination of the BRDF over a short period of time (30 days)
- 2 wavelengths in the visible range *(670 nm and 865 nm)*
- Operational processing line providing the required products (k_1 and k_0)

2.2 Aerodynamic length and POLDER protrusion coefficient

Aerodynamic roughness length estimated or measured over desert areas were compared to the POLDER protrusion coefficient for a large range of surface roughness (Marticorena et al., in press). An empirical relationship has been established between these two parameters :

$$\Rightarrow \quad k_1/k_0 = 0.052 \ln(Z_0) + 0.277 \qquad (1)$$

2.3 Data set composition

The establishment of a protrusion coefficient map over Asia (35.5° N - 47°N ; 73° E- 116° E) with a good level of confidence requires a **selection and a composition** of the available data sets.

Problem	Consequence	Solution
Clouds	Missing data	Composition of data sets for several months and two wavelengths (670 and 865 nm)
No correction for tropospheric aerosol in the processing line	Noisy signal	Selection of data set for periods of low dust emissions (winter) → Nov 96, Dec 96, Jan 97, Feb 97
Quality of the monthly data sets	Noisy signal and/or not representative	Selection as a function of the → Signal to noise ratio : IQ >5 → Number of observations used to fit the BRDF : N_{obs} > 100
Representativity of the composite data set	High standard deviation	Rejection of the data out of the range : med +/- std and N_{data} < 3

2.4 Validation of the protrusion map

The full resolution composite data set of k_1/k_0 is presented in figure 1. Due to the persistance of clouds, a lot of data are missing, especially in the northern part of the map. The main sandy deserts are characterized by low values of k_1/k_0, while the highest values are observed in the mountain ranges surrounding the Taklamakan desert and in the Tibetan plateau.

For five regions in the Chinese deserts, the map of k_1/k_0 is consistent with the geomorphological interpretation of high resolution Landsat images established by Walker et al. [2001].

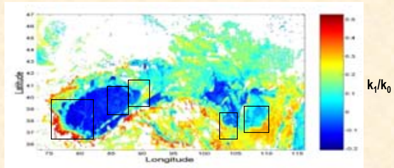

Figure 1

In order to test the spatial consistency of the information provided by the protrusion coefficient, the values obtained for different surface types (Table 1) and for sandy areas (Table 2) were examined.

From these two comparisons, we conclude that the POLDER k_1/k_0 map is consistent with observations, since :

⇨ **k_1/k_0 increases with the surface roughness ;**

⇨ **Similar surface types exhibit the same range of k_1/k_0.**

Surface type	k_1/k_0
Muntain range	0.43
Loess plateau	0.32
Stony desert	0.12
Stony desert	0.10
Vegetated sandy land	0.05
Sand dunes	-0.08
Sandy silty deposit	-0.13

Table 1

Location	k_1/k_0
Mu Us	0.05
Qubqi	-0.06
Ulan Buh	-0.06
Tengger	-0.05
Badain Jaran	-0.07
Qaidam - Kuntaq	-0.07
N.E Taklamakan	-0.09
SW Taklamakan	-0.11

Table 2

2.5 Map of the roughness length and erosion threshold

From the composite map of k_1/k_0 at the resolution of ¼°× ¼° and the equation (1), a map of roughness length was established (Figure 2 a). Based on the model from Marticorena and Bergametti [1995] and assuming a logarithmic wind velocity profile, the 10m threshold wind velocities were estimated (Figure 2 b).

Figure 2

(a) (b)

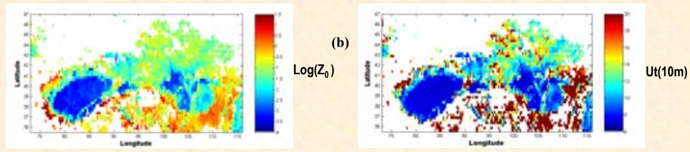

3. DUST EVENT FREQUENCY IN “ DRY ” CONDITIONS

The estimated erosion threshold allows the simulation of the dust event frequency, i.e. the number of times the wind velocity exceeds the erosion threshold. Dust event frequencies were simulated using the 1°× 1° ECMWF analyzed surface wind fields interpolated at the ¼°× ¼° resolution in “dry” conditions (i.e. without accounting for the inference of the soil moisture). Only the most intense simulated dust events (dust flux >10^{-9} g.cm^{-2}.s^{-1}, for a standard desert soil : fine sand) were selected.

4.1 Two main sources of dust events

The average simulated frequencies in percent (Figure 3) for three years (1997-1999) indicates two main sources of dust events : the Taklamakan in the west and the deserts of the north of China.

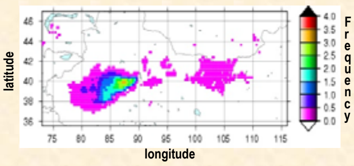

Figure 3

The frequencies of dust storms (horizontal visibility < 1 km and relative humidity <60%) derived from the daily measurements of the Chinese meteorological stations globally indicate the two same source regions of dust events, with the highest of dust storm frequency is observed in the southwestern Taklamakan.

Moreover, we compared the average simulated frequencies, for the three years studied, with the TOMS Aerosol Index (Herman et al., 1997) averaged over the same period at the 1°x1.25° spatial resolution (Figure 4).

Both the simulations and the TOMS AI show that the dust event frequencies are higher in the Taklamakan than in the eastern deserts. The highest simulated dust event frequencies and the highest value of the TOMS AI are located in the same region of the Taklamakan desert.

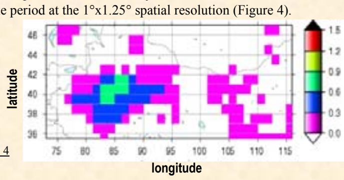

Figure 4

4.2 Variability of the interannual simulations in the Taklamakan

From 1997 to 1999, annual distributions of simulated average dust event frequencies were compared with the average TOMS AI in the Taklamakan region (Figure 5).

Globally, the maxima are simulated and observed during the same period, i.e. in late spring. Both the TOMS AI and the simulations show a more pronounced seasonal cycle in 1998 and 1999 than in 1997. Moreover, the frequencies of the simulated emissions and the TOMS AI are more important at the end of the summer and in the autumn of 1997 than the other years.

Figure 5

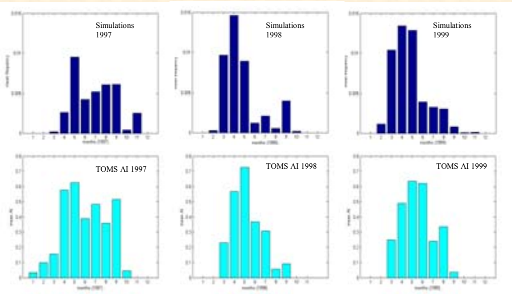

The overestimations of November 1997, March 1998 and March 1999 simulations and the underestimations of April 1997, June 1998 and June1999 can be noticed.

4. SENSITIVITY

5.1 Soil moisture influence

Soil moisture was computed using the 1°× 1° ECMWF meteorological fields (precipitation, temperature, albedo), and the soil texture profiles derived from the 1°× 1° FAO map (Zobler, 1986 ; Webb et al., 2000). The increase in the wind erosion thresholds as a function of the soil moisture (Fécan et al., 1999) was accounted for in the simulation of dust event frequencies. Figure 6 presents the mean difference in percent between the “dry” and “wet” averages simulated frequencies for three years (1997-1999).

The soil moisture influence is important in the southwestern Taklamakan, and spatially limited in the southwestern of the deserts of the north of China. Thus, the soil moisture does not change the relative contribution of the two main sources of dust events.

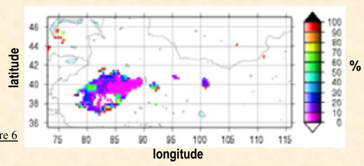

Figure 6

Figure 7 represents the monthly difference between “dry” and “wet” simulated emission frequencies in the Taklamakan. The differences are smaller than 30 percent except for November 1997, and the seasonal cycle is globally unchanged. The influence of soil moisture does not decrease the peaks of March 1998 and March 1999.

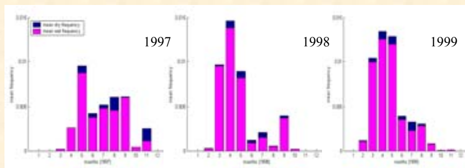

Figure 7

5.2 Dust flux threshold

In order to test the sensitivity of the simulated frequencies to the dust flux threshold, we compared, for three years (1997-1999), the dry relative simulated emission average frequencies/month for different flux thresholds (Figure 8) :

- dust flux > 10^{-10} g.cm^{-2}.s^{-1}
- dust flux > 5.10^{-10} g.cm^{-2}.s^{-1}
- dust flux > 10^{-9} g.cm^{-2}.s^{-1}

the same standard soil (fine sand) was applied for whole the studied area.

Figure 8

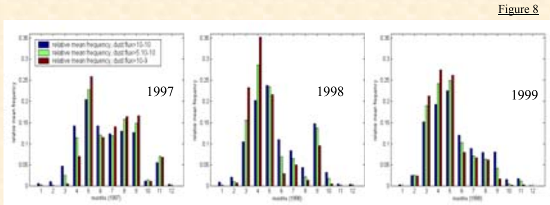

Stronger the flux condition is, more important the gaps of the relative simulated emission average frequencies/month are. For March 1997, April 1997 and June 1998, the relative decrease is important. On the other hand, for March 1998 and April 1998 a strong increase is observed.

These results suggest that the seasonnal pattern of the dust event frequency cannot be assessed independently of the dust emission intensity.

5. CONCLUSION

The POLDER protrusion coefficients k_1/k_0 allows the retrieval of the aerodynamic roughness length over desert areas, which represents a key parameter for the simulation of desert dust emissions. Such k_1/k_0, parameter globally available at the ~6 km × 6 km resolution, enables the establishment of regional and/or global simulation maps.

Both the localisation of the main sources and the variability of inter-seasonal cycle of the dust event frequencies simulated for the Chinese deserts using POLDER k_1/k_0 are in reasonable agreement with the TOMS AI.

However, a quantitative comparison requires the computation of the dust emission fluxes. Such a computation must account for the different surface types encountered in arid and semi arid areas.

Such an approach will be used on a global k_1/k_0 dataset, which should improve the simulation of the desert dust emissions and thus the assessment of their impacts on a global scale.